analytical chemistry

Article

pubs.acs.org/ac

Open Circuit (Mixed) Potential Changes Upon Contact Between Different Inert Electrodes—Size and Kinetic Effects

Jun Hui Park,[†] Hongjun Zhou,[†] Stephen J. Percival,[‡] Bo Zhang,[‡] Fu-Ren F. Fan,[†] and Allen J. Bard*[,†]

[†]Center for Electrochemistry, Department of Chemistry and Biochemistry, The University of Texas at Austin, Austin, Texas 78712, United States

[‡]Department of Chemistry, University of Washington, Seattle, Washington 98195, United States

ABSTRACT: We investigate the principle of the open circuit potential (OCP) change upon a particle collision event based on mixed potential theory and confirmed by a mimic experiment in which we studied the changes in the OCP when two different electrodes (Pt and Au) are brought into contact in a solution that contains some irreversible redox couples. A micrometer-sized Au ultramicroelectrode, when connected in parallel to a Pt micro- or nanoelectrode, showed clearly measurable OCP changes whose magnitude matches well with that predicted by a simplified mixed potential theory for a pair of different electrode materials. On the basis of the study, each electrode establishes a different mixed potential involving two or more half reactions that have different heterogeneous electron transfer kinetics at different electrodes and the OCP changes are very sensitive to the relative ratio of the rate constant of the individual half reaction at different materials.

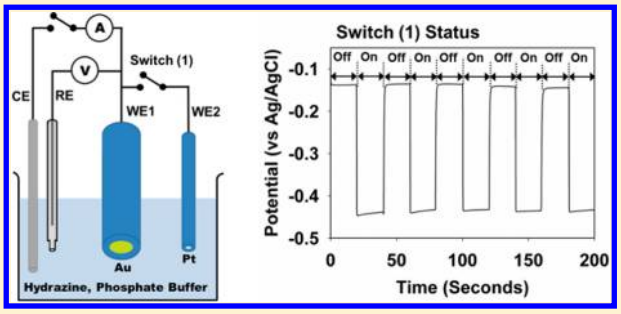

We discuss here the changes in the open circuit potential (OCP) when two different electrodes (e.g., Pt and Au) are brought into contact in a solution that does not contain reversible redox species. Under these conditions, a different mixed potential involving two or more half reactions is established at each electrode that depends on the heterogeneous electron transfer kinetics. The OCP changes when the two electrodes are contacted in a manner that is very sensitive to small changes in half reaction rates, so that one can dectect collisions of nanometer size particles on micrometer size ultramicroelectrodes (UMEs).

We have recently demonstrated single nanoparticle (NP) detection based on a potentiometric technique by measuring the OCP at an UME.[1] The OCP exhibits stepwise changes at the working electrode (e.g., a Au UME) with time, when a solution of NPs (e.g., Pt NPs) are injected into the electrochemical cell containing irreversible redox reactions (e.g., involving reduction of protons and oxidation of hydrazine). The OCP change is related to the kinetics of the redox processes, the concentration of the redox species, the NP size, and the UME size. Earlier we reported similarly shaped current steps when measuring the current at a constant potential under the same conditions; these have been ascribed to the sticking of individual Pt NPs on the Au UME after the collision where they electrocatalyze the hydrazine oxidation reaction.[2−5]

In the potentiometric method,[1] before the Pt NPs contact the Au UME, charge transfer can occur between each Pt NP and the solution containing hydrazine and protons to attain a NP OCP. Similar charge transfer occurs at the Au UME to establish an OCP. After the Pt NPs collide and stick to the Au UME, the current balance is changed and a new steady state is established via capacitive charging and the charge transfer reactions between Pt NPs, the Au UME, and redox species. This causes a shift in OCP in a sharp transition producing a series of potential steps. The OCP seen with a reversible redox couple produces a poised solution, where kinetically the two half reactions (anodic and cathodic) of the same redox couple establish the thermodynamically expected potential, at the point where the external current is, by definition, zero. The analogous situation occurs when there is not a single reversible redox couple that establishes the electrode potential but where two or more different half-reactions combine to produce a net zero external current to establish the potential, a so-called mixed potential. This concept was first described by Wagner and Traud[6] and has largely been used in corrosion science.[7,8] However, the same concept can be applied to catalytic systems, for example, in treating metal catalysis of solution redox reactions.[9,10] In these applications, however, the redox reaction (e.g., the corrosion reaction) is spontaneous, implying that $E^{o}_{Ox} - E^{o}_{Red} < 0$ (where E^{o}_{Ox} and E^{o}_{Red} are the standard potentials for the oxidant and reductant half-reactions). This usually produces a significant mixed or half-reaction current, i_m (also called the corrosion current) at the OCP (also called the corrosion potential) (Figure 1a). The situation of interest here is different in that either $E^{o}_{Ox} - E^{o}_{Red} > 0$ (as would be the case, for example, for the open circuit potential of a Pt electrode in deaerated 1 M

Received: September 7, 2012
Accepted: December 14, 2012
Published: December 14, 2012

 © 2012 American Chemical Society dx.doi.org/10.1021/ac3025976 | *Anal. Chem.* 2013, 85, 964−970

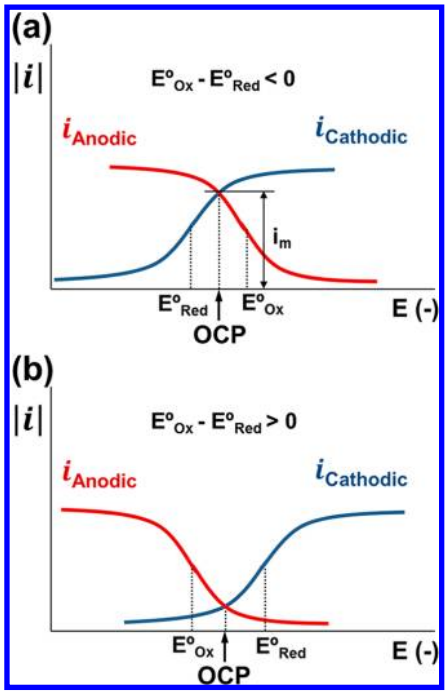

Figure 1. Schematic representation of the half reaction $i-E$ curves (a) $E^{\circ}_{Ox} - E^{\circ}_{Red} < 0$ and (b) $E^{\circ}_{Ox} - E^{\circ}_{Red} > 0$.

H_2SO_4) (Figure 1b) or if the reaction is spontaneous but involves very slow kinetics. In this case, the half-reaction current is very small and the mixed potential depends strongly on small changes in half-reaction kinetics and, in some cases, mass transport (where the size and shape of the electrodes and diffusion coefficients are considered).

We provide here a theoretical basis for this potentiometric technique for single NP detection. To mimic the particle collision experiment, we also show experiments in which the OCPs of Pt UMEs or nanoelectrodes of different sizes are measured alone and when connected to different-size Au UMEs.

EXPERIMENTAL SECTION

Reagents. Sodium phosphate dibasic anhydrous (Na_2HPO_4), sodium phosphate monobasic monohydrate ($NaH_2PO_4{\cdot}H_2O$), and calcium chloride anhydrous ($CaCl_2$) were obtained from Fisher Scientific (Pittsburgh, PA). All other chemicals were obtained from Sigma or Aldrich, unless otherwise stated. Hydrazine anhydrous (N_2H_4) was obtained from Sigma-Aldrich. All chemicals were used as received. Millipore water (>18 MΩ) was used in all experiments. Platinum (99.99%) and gold (99.99%) wires, 25 and 10 μm diameter, from Goodfellow (Devon, PA) were used to fabricate the UMEs.

Preparation of Ultramicroelectrodes. Pt and Au UMEs were prepared following the general procedure developed previously. Briefly, a 10 μm or a 25 μm metal (Au, Pt) wire was sealed in glass after rinsing with ethanol and water. Pt wire (2 μm diameter) is obtained from the electrochemical etching of a 25 μm wire in the etching solution (saturated $CaCl_2$/concentrated HCl/water = 60:4:36 by volume %). The electrode was then polished with an alumina powder water suspension to a mirror finish. The surface area was checked with standard redox electrochemistry of ferrocene methanol. The Pt nanoelectrode was fabricated by a method reported elsewhere.[11]

Instrumentation. The electrochemical experiments were performed using a CHI model 630 potentiostat (CH Instruments, Austin, TX) with the three-electrode cell placed in a Faraday cage. A 3 mm diameter carbon rod was used as the counter electrode (CE), and the reference electrode (RE) was Ag/AgCl in saturated KCl solution and all potentials are quoted vs this RE. No filters were selected for potential, current, and current converter in the CHI software. A laser puller (P-2000, Sutter Instrument Company) was used for the preparation of the Pt nanoelectrodes.

Switching Device. A push button switch DS-196 (single pole-double throw, Miyama electronic parts, Japan) was used for making a connection between the Au and Pt electrodes. The Au electrode and the working electrode cable were connected to the pole. The Pt electrode was connected to the other switch contact (Scheme 1). Thus by opening and closing the switch, one can select either Au or Au + Pt as the working electrode.

Scheme 1. Pictorial Representation of the Experimental Setup of Parallel Connected Different Electrode Materials to Mimic the Single Pt Nanoparticle Collision Event on Au Electrode

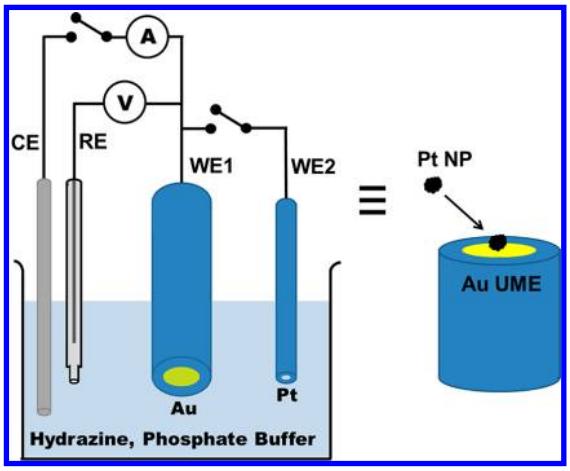

Pretreatment. Before every experiment, the solution was deaerated with Ar and all electrodes were polished prior to use with alumina (0.05 μm) paste on microcloth pads (Buehler, Lake Bluff, IL). The Au UME was subjected to a few potential cycles between 0.4 and −0.8 V. The OCP was measured with respect to time with the input impedance of the measuring circuit of 1 teraohm.

EXPERIMENTAL RESULTS

The OCP changing when two different metal electrodes are connected was widely investigated in the early days of electrochemistry, especially in connection with galvanic processes and corrosion.[12] In these studies, a significant current flows when the two metals are connected, e.g., the classic experiment of Zn connected to Pt, where the oxidation of Zn is promoted by the occurrence of proton reduction on the Pt. However in descriptions of these experiments, it was noted that "gold and platinum [connected] together produce no current"[13] implying that the potential changes are very small. There have perhaps been more detailed studies of the connection of inert or noble metal (or carbon) electrodes in

dx.doi.org/10.1021/ac3025976 | Anal. Chem. 2013, 85, 964−970

various solutions, but we have not been able to find them. To mimic the OCP changes seen when Pt NPs stick on a Au UME, we have simply used Pt and Au UMEs of different diameter (nanometer to micrometer) using the apparatus in Scheme 1, measuring the potential with an electrochemical workstation or an electrometer with respect to a Ag/AgCl reference electrode.

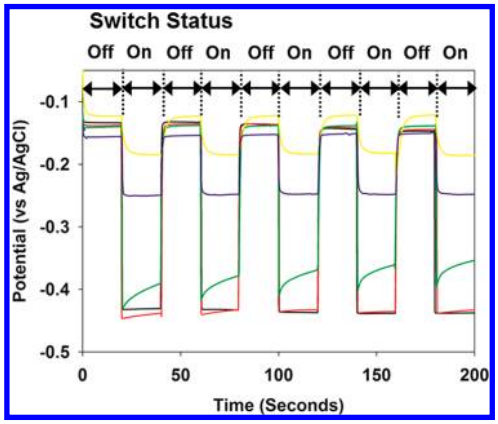

Figure 2. OCP vs time plots for 12.5 μm radius Au UME connected with 12.5 μm (black line), 5 μm (red line), 1 μm (green line), 50 nm (blue line), and 20 nm (yellow line) radius Pt electrode in the presence of 5 mM phosphate buffer (pH 7) and 15 mM hydrazine. The connection was controlled by a switch, and the switch status changes every 20 s. Data acquisition time is 100 ms.

Figure 2 and Table 1 show dynamic changes of OCP when Pt electrodes of various sizes (radii 20 nm to 12.5 μm) are connected to an Au UME (radius 12.5 μm) in a 5 mM phosphate buffer (pH 7) containing 15 mM hydrazine. Upon connecting the Au electrode to Pt, the OCP shifts to more negative values; when the switch is opened and only the Au electrode is connected as a working electrode, the OCP shifts back to OCP of Au. The switch status changed every 20 s. The change in OCP, ΔE_{OCP}, was larger for larger Pt electrodes (>300 mV) and decreased to about 60 mV with a 20 nm radius Pt. This result demonstrates that the OCP in hydrazine system is very sensitive to single Pt NP detection and that the OCP of Pt can be obtained from partial coverage of Pt on an Au UME.

By opening and closing the switch we can see reversible potential changes, although the OCP of Pt and Au changed slightly with time, probably because of surface contamination by impurities as reported previously.[1] The OCP may also be affected by reaction intermediates or products adsorbed on metal surface.[14,15] Connected Pt nanoelectrode took a few seconds to reach a steady OCP, that is also a function of the Pt pretreatment; these characteristics were also shown with Pt NP collisions. However, with a microscale Pt electrode, it instantly reaches the steady state potential. To stay at OCP conditions, charge moves between the Pt electrode, Au electrode, and redox species. The delay time seemed to be related with the magnitude of the exchange current at the Pt electrode.

Figure 3 shows another example of OCP change at a Au UME (radius, 5 μm) after connection with Pt electrodes in the

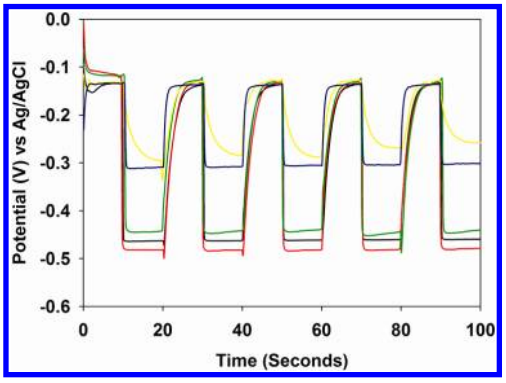

Figure 3. OCP vs time plots for 5 μm radius Au UME connected with 12.5 μm (black line), 5 μm (red line), 1 μm (green line), 50 nm (blue line), and 20 nm (yellow line) radius Pt electrode in the presence of 5 mM phosphate buffer (pH 7) and 15 mM hydrazine. The connection is controlled by a switch, and the switch status changes every 10 s. Data acquisition time is 100 ms.

presence of 5 mM phosphate buffer (pH 7) and 15 mM hydrazine. The OCP change of the Au UME (radius, 5 μm) is larger than that of a Au UME (radius, 12.5 μm) when the Pt nanoelectrode is connected. The comparative size of Au and Pt is actually related to OCP changes. In this case, we used 10 s intervals to change the switch status. As shown in Figures 2 and 3, a Pt nanoelectrode takes a few seconds to reach a steady state.

The potential change is not linearly proportional to the size of the Pt electrode. Similarly with a constant potential bias, the magnitude of the collision current step is proportional to the radius of the spherical particle, independent of Au electrode size. Instead, the OCP shows a more complicated relation with the radius of the Pt electrode. We explain this relation based on mixed potential theory of a two electrode system.

THEORY ANALOGOUS TO THE AU PT/HYDRAZINE SYSTEM

We present here a simplified treatment of the mixed potential at a pair of different electrode materials analogous to the experiments described above. This captures the essential elements of the theory. We present a more general model in the next section. In the simplified model, we assume that the potential of the electrodes are controlled by a single cathodic half-reaction current, e.g., for proton (or water) reduction ($2H^+ \rightarrow H_2 + 2e$) and a single anodic half reaction current, e.g., for hydrazine oxidation ($N_2H_4 \rightarrow N_2 + 4H^+ + 4e$). In fact,

Table 1. OCP Change (From Experiment and Computation) of 12.5 and 5 μm Radius Au UME after Connection with Various Sizes of Pt Electrode in the Presence of 5 mM Phosphate Buffer (pH 7) and 15 mM Hydrazine

12.5 μm Au connected to	12.5 μm Pt	5 μm Pt	1 μm Pt	50 nm Pt	20 nm Pt
OCP change (experiment)	298 mV	306 mV	263 mV	94 mV	62 mV
OCP change (computed)	299 mV	290 mV	240 mV	95 mV	46 mV
5 μm Au connected to	12.5 μm Pt	5 μm Pt	1 μm Pt	50 nm Pt	20 nm Pt
OCP change (experiment)	332 mV	363 mV	325 mV	175 mV	162 mV
OCP change (computed)	324 mV	319 mV	287 mV	142 mV	96 mV

dx.doi.org/10.1021/ac3025976 | Anal. Chem. 2013, 85, 964−970

additional reactions may occur, for example, the reduction of residual oxygen or the oxidation of trace impurities, but these are neglected. We indicate the cathodic half-reaction by subscript C (and the reactant as O) and the anodic half-reaction by subscript A (and the reactant as R). Note that the actual kinetics of these inner sphere electrode reactions are usually complicated and multistep. Thus we assume a Butler–Volmer formalism and neglect mechanistic complications. The intention here is simply to demonstrate that with appropriately estimated kinetics and potentials, one can detect OCP changes when nanometer particles are in contact with micrometer electrodes. We do not intend to represent the actual kinetics of the half reactions.

We can represent the half-reaction currents, i_C and i_A, as[16]

$$|i_C| = n_C F A_j k_C^o C_O(x=0) \exp[-\alpha_C f(E - E_C^o)] \quad (1)$$

$$|i_A| = n_A F A_j k_A^o C_R(x=0) \exp[(1-\alpha_A) f(E - E_A^o)] \quad (2)$$

A_j is the area of the electrodes (j = 1 (Au) or 2 (Pt)), k_C^o, k_A^o, are the apparent rate constants in the heterogeneous rate expression and depend on electrode composition. $C_O(x=0)$ and $C_R(x=0)$ are the concentrations of O (e.g., H^+) and R (e.g., N_2H_4) at the electrode surface, E_C^o and E_A^o are the assumed standard potentials of the overall half-reactions, and $f = F/RT$.

One can express the concentrations at the electrode surface in terms of measurable variables as

$$C_O(x=0) = C_O^*[1 - i_C/i_{dC}] \quad (3)$$

$$C_R(x=0) = C_R^*[1 - i_A/i_{dA}] \quad (4)$$

where C_O^* and C_R^* are the bulk concentrations of O and R, and $i_{d,C}$ and $i_{d,A}$ are the mass transfer controlled limiting currents that can be written in terms of mass transfer coefficients m_O and m_R, which are functions of the size and shape of the electrodes.

$$|i_{dC}| = n_C F A_j m_O C_O^* \quad (5)$$

$$|i_{dA}| = n_A F A_j m_R C_R^* \quad (6)$$

Combining these equations results in the final general expressions

$$|i_C| = (k_C^o/m_O)(i_{dC} - i_C) \exp[-\alpha_C f(E - E_C^o)] \quad (7)$$

$$|i_A| = (k_A^o/m_R)(i_{dA} - i_A) \exp[(1-\alpha_A) f(E - E_A^o)] \quad (8)$$

For the special case where mass transfer effects can be neglected, so $C_O(x=0) \approx C_O^*$ and $C_R(x=0) \approx C_R^*$, and $i_{dC} \gg i_C$ and $i_{dA} \gg i_A$, these equations become

$$|i_C| = (k_C^o/m_O) i_{dC} \exp[-\alpha_C f(E - E_C^o)] \quad (7A)$$

$$|i_A| = (k_A^o/m_R) i_{dA} \exp[(1-\alpha_A) f(E - E_A^o)] \quad (8A)$$

OCP at a single electrode, i.e., $E = E_{OCP}$, occurs when the external current is zero, or $|i_C| = |i_A|$. Note that we take the sign of cathodic current as positive (i_C) and anodic current negative (i_A). This results in the equation

$$E_{OCP} = \frac{\ln\left[\frac{(k_C^o/m_O) i_{dc}}{(k_A^o/m_R) i_{dA}}\right] + f[(1-\alpha_A)E_A^o + \alpha_C E_C^o]}{f(1 - \alpha_A + \alpha_C)} \quad (9)$$

With the approximation $\alpha_C = \alpha_A = \alpha$, this becomes

$$\left(\frac{RT}{F}\right) \ln\left[\frac{(k_C^o/m_O) i_{dc}}{(k_A^o/m_R) i_{dA}}\right] + (1-\alpha)E_A^o + \alpha E_C^o = E_{OCP} \quad (10)$$

Note this equation does not contain the mass transfer terms, since by introducing the definitions of the limiting currents, eqs 5 and 6, we obtain

$$\left(\frac{RT}{F}\right) \ln\left[\frac{k_C^o n_C C_O^*}{k_A^o n_A C_R^*}\right] + (1-\alpha)E_A^o + \alpha E_C^o = E_{OCP} \quad (11)$$

In this case, E_{OCP} is independent of the electrode area, A_j.

However to treat E_{OCP} for the coupled electrodes, the condition is

$$|i_{C,j=1}| + |i_{C,j=2}| = |i_{A,j=1}| + |i_{A,j=2}| \quad (12)$$

This requires using expressions for the individual half-reaction currents. Equations 7 and 8 can be rearranged to yield suitable expressions for $|i_C|$ and $|i_A|$

$$|i_C| = i_{dC} \Big/ \left\{1 + \frac{m_O}{k_C^o} \exp[\alpha_C f(E - E_C^o)]\right\} \quad (13)$$

$$|i_A| = i_{dA} \Big/ \left\{1 + \frac{m_O}{k_C^o} \exp[-(1-\alpha_A) f(E - E_A^o)]\right\} \quad (14)$$

These expressions can be used with the suitable parameters for each electrode and half-reaction to calculate curves for the four currents, $|i_{C,j=1}|$, $|i_{C,j=2}|$, $|i_{A,j=1}|$, $|i_{A,\,j=2}|$ as functions of E. The summation of currents $|i_{C,j=1}| + |i_{C,j=2}|$ and $|i_{A,j=1}| + |i_{A,\,j=2}|$ can then be plotted and where eq 12 is satisfied, $E = E_{OCP}$. Figure 4

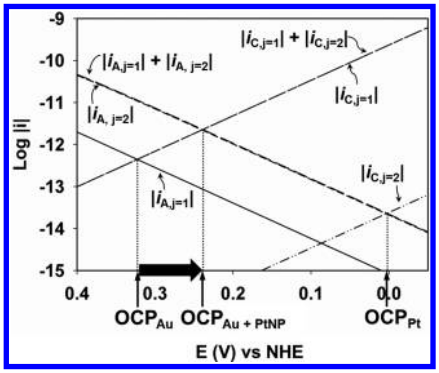

Figure 4. Simulated series of anodic current and cathodic current vs potential plot of Au disk electrode (j = 1) and Pt spherical nanoparticle (j = 2). OCP is decided by definition; net current equal zero ($|i_{A,\,j}| = |i_{C,\,j}|$). OCP of two electrode materials ($OCP_{Au+PtNP}$) is decided when eq 12 is satisfied. The large arrow represents the OCP shift upon contact with Pt NP to an Au UME. (Au disk radius, 12.5 μm; Pt nanoparticle radius, 20 nm).

shows a representative example for the case of a disk electrode ($m_{O,1} = 4D_O/\pi r_1$ and $m_{R,1} = 4D_R/\pi r_1$) and a spherical nanoparticles ($m_{O,2} = D_O/r_1$ and $m_{R,2} = D_R/r_2$). The intersection point of the $|i_j|$–E plot (or $\log|i_j|$–E plot) indicates the OCP where net current equals zero ($|i_{A,\,j}| = |i_{C,\,j}|$). Equivalently, one can solve these equations to find E_{OCP} directly, but the equation is cumbersome.

We should stress that, as in most treatments of complex inner sphere heterogeneous electron reactions, the actual rate expressions depend on knowledge of the reaction mechanism, so those given here, especially in terms of the overall reaction

dx.doi.org/10.1021/ac3025976 | Anal. Chem. 2013, 85, 964–970

E^{o}, can only be considered "effective" ones. Moreover, although we do not suggest this approach is a good one for determining kinetic parameters for electrode reactions, one cannot within this formalism separate the k^{o} and E^{o} values, e.g., in eqs 13 and 14. A reviewer suggested that to prevent any confusion along these lines, they be combined into a single new variable. Thus one can equivalently express the equations as shown in eqs 15 and 16:

$$k_C = k_C^{o} \exp(\alpha_C f E_C^{o}) \exp(-\alpha_C f E) = \kappa_C \exp(-\alpha_C f E) \quad (15)$$

$$k_A = k_A^{o} \exp[(1-\alpha_A) f E_A^{o}] \exp[(1-\alpha_A) f E] = \kappa_A \exp[(1-\alpha_A) f E] \quad (16)$$

where κ_C and κ_A are constants containing the k^{o} and E^{o} terms.

Equations 13 and 14 can be simplified to

$$|i_C| = i_{dC} \Big/ \left\{1 + \frac{m_O}{k_C}\right\} \quad (17)$$

$$|i_A| = i_{dA} \Big/ \left\{1 + \frac{m_O}{k_A}\right\} \quad (18)$$

This approach can be used to show how E_{OCP} depends on the electrode sizes (r_1 and r_2) and heterogeneous rate constants ($k^{o}_{C,1}$, $k^{o}_{C,2}$, $k^{o}_{A,1}$, $k^{o}_{A,2}$) and E^{o} values (or equivalently the κ_C and κ_A values). Figures 5 and 6 shows the Pt electrode size

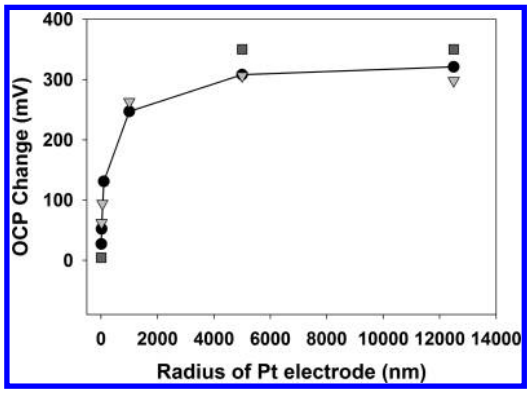

Figure 5. Experimental OCP change (square, triangle plot) and computed OCP change (circle plot with solid line) of 12.5 μm radius Au UME is plotted after connection with various sized Pt electrode in the presence of 5 mM phosphate buffer (pH 7) and 15 mM hydrazine (triangle plot) 50 mM phosphate buffer (pH 7) and 15 mM hydrazine (square plot).

effect on the OCP change of 12.5 and 5 μm radius Au disk electrodes from a mixed potential theory computation. The theoretical plot matches the two sets of experimental results when the heterogeneous rate constants with the assumed standard potentials are adjusted. With given parameters (i.e., reactant concentration, diffusion coefficient, alpha, and standard potential), the ratio of anodic and cathodic rate constant($k^{o}_{A,j}/k^{o}_{C,j}$) controls the OCP of each electrode material. The size of the electrode does not affect the OCP of that single material electrode. The OCP change after connection with a different electrode material reflects the kinetic (rate contant) differences at the different materials. The essence of the highly sensitive system mainly relies on the heterogeneous catalytic effect of anodic and cathodic reactions. In this system, we take the anodic reaction rate constant at Pt ($k^{o}_{A,1}$) to be much larger

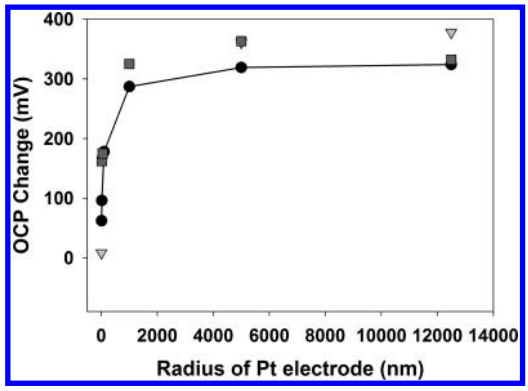

Figure 6. Experimental OCP change (square, triangle plot) and computed OCP change (circle plot with solid line) of 5 μm radius Au UME is plotted after connection with various sized Pt electrode in the presence of 5 mM phosphate buffer (pH 7) and 15 mM hydrazine (triangle plot) 50 mM phosphate buffer (pH 7) and 15 mM hydrazine (square plot).

than that at Au ($k^{o}_{A,2}$), while we take the cathodic reaction rate constants of Pt ($k^{o}_{C,1}$) and Au ($k^{o}_{C,2}$) to be closer. The OCP of each electrode material is fixed, but a high ratio of anodic rate at two material ($k^{o}_{A,1}/k^{o}_{A,2}$) (j = 1, Au; j = 2, Pt) the joint OCP on connection or adhesion is significant, even with a large difference in the size of the electrodes. Detailed parameters for the calculation are shown in Table 2. The theoretical results

Table 2. Simulation Parameters for Computed OCP Plot in Figures 4–7[a]

C_R^{*} (M)	0.015
C_O^{*} (M)	0.005
D_R (cm^2/s)	1×10^{-5}
D_O (cm^2/s)	1×10^{-5}
radius of Au disk UME (cm)	1.25×10^{-3}
radius of Pt sphere (cm)	2×10^{-6}
k_C^{o} (cm/s) of Au	1×10^{-4}
k_A^{o} (cm/s) of Au	4×10^{-8}
k_C^{o} (cm/s) of Pt	0.01
k_A^{o} (cm/s) of Pt	0.1
α_C	0.5
α_A	0.5
E_C^{o} (V vs NHE)	0
E_A^{o} (V vs NHE)	0.3

[a]Radius of electrodes and type (disk or sphere) of electrodes differ in each case.

are compared with two experimental data sets with 12.5 and 5 μm radius Au disk electrodes. Although two experiments involved slightly different experimental buffer capacities, the OCP change was about the same. The experimental data shown in Figures 5 and 6 matched well with theory.

This model and the experiments with UMEs suggests that the OCP changes upon particle collision events[1] can be modeled as a spherical electrode connected to a disk electrode. In Figure 7, the solid line shows computed potential changes in which the kinetic parameters are identical with those in Figures 5 and 6. The two trianglular points represent the first potential step found with an actual Pt NP (2 and 16 nm radius) collision event on an Au UME (5 μm in radius). The difference in the experimental OCP shifts and the computed value is surprisingly small, considering the large number of adjustable parameters

dx.doi.org/10.1021/ac3025976 | Anal. Chem. 2013, 85, 964–970

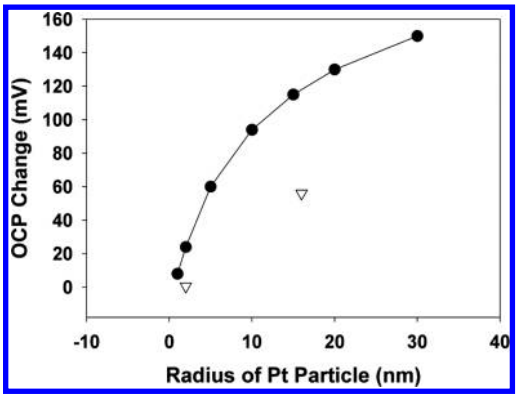

Figure 7. Experimental OCP change (triangle plot) and the computed OCP change (solid circles and solid line) of 5 μm radius Au UME is plotted after connection with spherical Pt NP (2 and 16 nm in radius) in the presence of 5 mM phosphate buffer (pH 7) and 15 mM hydrazine (16 nm in radius Pt NP), 50 mM phosphate buffer (pH 7), and 15 mM hydrazine (2 nm in radius Pt NP).

that go into the calculation. The Pt NP surface is also partially blocked by adsorbed citrate, which can affect the rate of a catalyzed reaction compared to the Pt disk electrode, which is cleaned by polishing and electrochemical pretrement. Uncertainty in the actual particle radius and Pt NP surface contamination by reaction intermediates are also factors in the observed OCP changes with NPs.

In principle, on the basis of this theoretical treatment, one can roughly estimate the relative rate of a given electrode reaction at one material by the OCP change found after connecting it to an electrode of a different material with a known rate constant. Finally, we might note that measurement of the OCP potential is simplest from an experimental viewpoint, but increased sensitivity could be obtained by application of a small constant current, e.g., for the example here, in the anodic direction.

GENERAL THEORY

The equations derived in Theory Analogous to the Au Pt/Hydrazine System can be generalized to take into account a greater number, N, of reactions possible at each electrode, indexed by i. Thus one considers a series of half reactions:

$$O_i + n_i e = R_i \quad i = 1, N \quad E_i^\circ \tag{19}$$

The electrodes are indexed by j and typically, as above, j = 1,2. However, if one wanted to model multiple electrodes or particles in contact to the larger UME, larger numbers could be accommodated. The particular parameters are then indexed by i and j, so the heterogeneous rate constant is $k_{i,j}^\circ$ and a given mass transfer coefficient is $m_{Oi,j}$. One can then generalize the equations in the preceding section, so that the general forms of eqs 1, 2, and 3 are

$$|i_{Cij}| = n_i F A_j k_{i,j}^\circ C_{Oi}(x = 0) \exp[-\alpha_{ij} f(E_j - E_i^\circ)] \tag{20}$$

$$|i_{Aij}| = n_i F A_j k_{i,j}^\circ C_{Ri}(x = 0) \exp[(1 - \alpha_{ij}) f(E_j - E_i^\circ)] \tag{21}$$

$$C_{Oi}(x = 0) = C_{Oi}^*(1 - i_{Cij}/i_{dCij}) \tag{22}$$

where i_{dCij} is the limiting cathodic current for species O_i at electrode j, given by

$$i_{dCij} = n_i F A_j m_{Oij} C_{Oi}^* \tag{23}$$

These equations lead to the general equations, equivalent to eqs 7 and 8

$$|i_{Cij}| = (k_{i,j}^\circ/m_{Oij})(i_{dCij} - i_{Cij}) \exp[-\alpha_{ij} f(E_j - E_i^\circ)] \tag{24}$$

$$|i_{Aij}| = (k_{i,j}^\circ/m_{Rij})(i_{dAij} - i_{Aij}) \exp[(1 - \alpha_{ij}) f(E_j - E_i^\circ)] \tag{25}$$

These lead to the final general forms of eqs 13 and 14:

$$|i_{Cij}| = i_{dCij}/\{1 + (m_{Oij}/k_{ij}^\circ) \exp[\alpha_{ij} f(E_j - E_i^\circ)]\} \tag{26}$$

$$|i_{Aij}| = i_{dAij}/\{1 + (m_{Rij}/k_{ij}^\circ) \exp[-(1 - \alpha_{ij}) f(E_j - E_i^\circ)]\} \tag{27}$$

The OCP condition is then found from all of the anodic and cathodic currents for two electrodes, with $E_j = E_{OCP}$:

$$\sum_{j=1}^{2} \sum_{i=1}^{N} |i_{Cij}| = \sum_{j=1}^{2} \sum_{i=1}^{N} |i_{Aij}| \tag{28}$$

CONCLUSIONS

Detection of Pt NP collision events on a Au UME by measuring its OCP changes is quantitatively explained by pairing in parallel different electrode materials analogous to the particle collision experiments. We present a simplified treatment of the mixed potential at a pair of different electrode materials. By adjusting the kinetic rate constants we can obtain a computed result which matches well with experimental results. The high sensitivity of the OCP to material is mainly due to the heterogeneous catalytic effects for the redox couples of two different oxidation and reduction reactions.

AUTHOR INFORMATION

Corresponding Author

*Fax: 512-471-0088. Phone: 512-471-3761. E-mail: ajbard@mail.utexas.edu.

Notes

The authors declare no competing financial interest.

ACKNOWLEDGMENTS

We appreciate support from the Robert A. Welch Foundation (Grant F-0021) and the National Science Foundation (Grant CHE-1111518) for support of the experimental studies (J.H.P., H.Z.). This work was also supported by the Department of Defense, Defense Threat Reduction Agency (Contract No. HDTRA1-11-1-0005) for the nanometer electrode preparation (S.J.P., B.Z.). The content of the information does not necessarily reflect the position or the policy of the federal government, and no official endorsement should be inferred.

REFERENCES

(1) Zhou, H.; Park, J. H.; Fan, F.-R.; Bard, A. J. *J. Am. Chem. Soc.* **2012**, *134*, 13212−13215.
(2) Xiao, X.; Bard, A. J. *J. Am. Chem. Soc.* **2007**, *129*, 9610−9612.
(3) Xiao, X.; Fan, F.-R. F.; Zhou, J.; Bard, A. J. *J. Am. Chem. Soc.* **2008**, *130*, 16669−16677.
(4) Xiao, X.; Pan, S.; Jang, J. S.; Fan, F.-R. F.; Bard, A. J. *J. Phys. Chem. C* **2009**, *113*, 14978−14982.
(5) Zhou, H.; Fan, F.-R. F.; Bard, A. J. *J. Phys. Chem. Lett.* **2010**, *1*, 2671−2674.
(6) Wagner, V. C.; Traud, W. *Z. Elektrochem.* **1938**, *44*, 391−402.
(7) Wagner, V. C.; Traud, W. *Corrosion* **2006**, *62*, 843−855.

(8) Zelinsky, A. G.; Pirogov, B. Y.; Yurjev, O. A. *Corros. Sci.* **2004**, *46*, 1083−1093.
(9) Spiro, M. *J. Chem. Soc., Faraday Trans. 1* **1979**, *75*, 1507−1512 and references therein.
(10) Miller, D. S.; Bard, A. J.; McLendon, G.; Ferguson, J. *J. Am. Chem. Soc.* **1981**, *103*, 5336−5341.
(11) Li, Y.; Bergman, D.; Zhang, B. *Anal. Chem.* **2009**, *81*, 5496−5502.
(12) Gmelin, L. *Handbook of Chemistry*; The Cavendish Society: London, 1848; Vol. *I*, 341−381.
(13) Gmelin, L. *Handbook of Chemistry*; The Cavendish Society: London, 1848, Vol. *I*, p 346.
(14) Aldous, L.; Compton, R. G. *Phys. Chem. Chem. Phys.* **2011**, *13*, 5279−5287.
(15) Bard, A. J. *Anal. Chem.* **1963**, *35*, 1602−1607.
(16) Bard, A. J.; Faulkner, L. R. *Electrochemical Methods: Fundamentals and Applications*, 2nd ed.; John Wiley and Sons: New York, 2001; Chapter 3.